J Oral Pathol Med (2004) 33: 177–84

www.blackwellmunksgaard.com/jopm

Basement membrane-type heparan sulfate proteoglycan (perlecan) and low-density lipoprotein (LDL) are co-localized in granulation tissues: a possible pathogenesis of cholesterol granulomas in jaw cysts

Manabu Yamazaki[1], Jun Cheng[1], Natsuko Hao[1,2], Ritsuo Takagi[2], Shiro Jimi[3], Hiroyuki Itabe[4], Takashi Saku[1]

[1]*Division of Oral Pathology, Department of Tissue Regeneration and Reconstruction,* [2]*Division of Oral and Maxillofacial Surgery, Department of Oral Health Science Niigata University Graduate School of Medical and Dental Sciences, 2-5274 Gakkocho-dori, Niigata 951-8514,* [3]*Department of Pathology, Fukuoka University School of Medicine, 7-45-1 Nanakuma, Johnan-ku, Fukuoka 814-0180, and* [4]*Department of Microbiology and Molecular Pathology, Faculty of Pharmaceutical Sciences, Teikyo University, Sagamiko 199-1095, Japan*

BACKGROUND: As perlecan contains a low-density lipoprotein (LDL) receptor-like repeats in the second domain of its core protein, LDL may be bound to perlecan, which is rich in granulation tissues. We wanted to study if this is the case in the cyst wall of radicular cysts, which are often associated with cholesterol granuloma.

METHODS: Thirty-three specimens of radicular cyst with cholesterol granulomas were immunohistochemically examined for comparative localizations of perlecan, apoprotein B (apo B), and oxidized LDL (Ox-LDL), and for mRNA expression levels for perlecan.

RESULTS: Myxoid or edematous stroma of immature granulation tissues was strongly positive for perlecan and simultaneously for apo B and Ox-LDL. Macrophages including foamy cells scattered in the granulation tissues were also immunopositive for Ox-LDL and occasionally for apo B. *In situ* hybridization showed that fibroblasts, endothelial cells, and pericytes had strong signals for perlecan, which was also confirmed by RT-PCR.

CONCLUSION: These results suggest that perlecan, which is abundantly produced and accumulated in the cyst wall of immature granulation tissue, traps Ox-LDL locally, and that Ox-LDL is phagocytosed by macrophages. Thus, LDL-laden foamy macrophages are aggregated in the granulation tissue, and free cholesterol from ruptured macrophages may be concentrated locally to be crystallized, which may induce foreign body granulomas in the cyst wall.

J Oral Pathol Med (2004) **33**: 177–84

Correspondence: Takashi Saku, Division of Oral Pathology, Department of Tissue Regeneration and Reconstruction, Niigata University Graduate School of Medical and Dental Sciences, 2-5274 Gakkocho-dori, Niigata 951-8514, Japan. Tel.: +81 25 227 2832. Fax: +81 25 227 0805. E-mail: tsaku@dent.niigata-u.ac.jp
Accepted for publication September 17, 2003

Keywords: cholesterol granuloma; heparan sulfate proteoglycan (HSPG); jaw cyst; low-density lipoprotein (LDL); LDL-receptor; perlecan

Introduction

Cholesterol granuloma is one of the most frequent histologic features of jaw cysts whether the cysts have inflammatory or developmental backgrounds (1). Cholesterol crystals are often found macroscopically in aspirated cystic fluids, which is also evidence that a cyst is in an inflammatory process (2). These crystals are represented in cholesterol clefts in tissue sections from paraffin-embedded blocks and are usually associated with foreign body reaction, which prolongs the inflammatory process of cyst walls (3). However, no histopathogenetic process of cholesterol granulomas has been clarified in this particular environment of the cyst wall.

In the process of our research efforts to study the functional roles of perlecan, a basement membrane-type heparan sulfate proteoglycan (HSPG) in pathophysiologic events, we have already shown that perlecan is expressed in the early phase of tissue remodeling in both neoplastic (4–12) and inflammatory (13–15) lesions. When perlecan is plentifully localized in either the stroma or the parenchyma, tissues commonly show a myxoid-type characteristic histologic feature (4, 5, 9–14). This may be explained by the fact that water molecules tend to aggregate around glycosaminoglycan chains of proteoglycans (16). Retention of water is one of the most characteristic functions of proteoglycans, which, for instance, results in the elastic property of cartilaginous tissues. The core protein of perlecan is composed of five domain structures. Its second domain contains repeated low-density lipoprotein (LDL) receptor consensus sequences (17, 18). Therefore, perlecan may function as an LDL receptor in the extracellular matrix.

Cyst walls are ideal for studying the organization process of granulation tissue because they have layered structures from inner immature to outer fibrous granulation tissues. During this maturation process, perlecan is thought to be deposited in the stroma. In addition, if perlecan functions as a receptor for LDL, LDL may be trapped in the stroma where perlecan is abundant. On the basis of the hypothesis that LDL is concentrated in perlecan-rich granulation tissue and concentrated cholesterol is crystallized in the cyst wall, we intended in this study to ascertain if there is co-expression of perlecan and LDL at the protein and mRNA levels in the cyst wall.

Materials and methods

Materials

Thirty-three surgical specimens of radicular cysts were collected for the present study from the surgical pathology files of the Division of Oral Pathology, Niigata University Graduate School of Medical and Dental Sciences, during a 2-year period from 1997 to 1998 after histopathologic examinations for cholesterol granulomas on tissue sections stained with hematoxylin and eosin or with toluidine blue. The samples were fixed in 10% formalin and routinely embedded in paraffin. Serial sections cut at 4 μm from paraffin blocks were used for immunohistochemical stainings and *in situ* hybridization. For reverse transcription-polymerase chain reaction (RT-PCR), four fresh surgical specimens of radicular cysts were obtained.

Antibodies

Mouse perlecan was prepared from the murine Engelbreth-Holm-Swarm (EHS) tumor, and the antibodies were raised in rabbits as described elsewhere (19). The anti-perlecan antibodies were used at a protein concentration of 50 μg/ml. Rabbit polyclonal antibodies against apoprotein B (apo B) of human LDL were obtained from Biogenesis Ltd. (Poole, UK; diluted at 1 : 75). A mouse monoclonal antibody to oxidized LDL (Ox-LDL; FOH1a/DLH3 clone (DLH3)) was generated as described elsewhere (20). A mouse monoclonal antibody to CD68 (PG-M1, Dako Ltd., Glostrup, Denmark; 1 : 100) was used to identify macrophages.

Immunohistochemistry

A peroxidase-anti-peroxidase (PAP) technique using goat anti-rabbit IgG (1 : 100; Cappel Laboratories, Cochranville, PA, USA) and rabbit PAP complex(1 : 100; Cappel) was employed for immunostaining for perlecan and apo B. For CD68, a streptavidin-biotin peroxidase technique using biotinylated rabbit anti-mouse IgG+IgA+IgM (Nichirei Co., Tokyo, Japan) and peroxidase-conjugated streptavidin (Nichirei Co.) was employed. For Ox-LDL immunohistochemistry with the DLH3 antibody, the avidin-biotin alkaline phosphatase technique using biotinylated rabbit anti-mouse IgM (Dako Ltd.) and alkaline phosphatase (ALP)-conjugated streptavidin (Vector Laboratories Inc., Burlingame, CA, USA) was employed. Deparaffinized sections stained for perlecan and apo B were first incubated with 6 mM periodic acid for 10 min and then with 3 mM sodium borohydride for 30 min at room temperature to block endogenous peroxidase activity. After washing with phosphate-buffered saline (PBS), the sections were digested with 3 mg/ml bovine testicular hyaluronidase (type I-S, 440 U/mg; Sigma Chemical Co., St Louis, MO, USA) in PBS for 30 min at 37°C. For CD68 immunostaining, the sections were digested with 1 mg/ml porcine pancreatic trypsin (Sigma Chemical Co.) in 0.05 M Tris–HCl, pH 7.6, containing 0.1% $CaCl_2$ for 15 min at 37°C. For Ox-LDL, the sections were pre-treated with 5 μg/ml pronase (Sigma Chemical Co.).

After enzymatic digestion, the sections were pre-incubated with 5% milk protein in PBS for 1 h to prevent non-specific protein binding. After overnight incubation with primary antibodies at 4°C, the sections were reacted with goat anti-rabbit IgG (1 : 100) or biotinylated rabbit anti-mouse immunoglobulins (1 : 300), followed by peroxidase–anti-peroxidase complex (1 : 500), peroxidase-conjugated streptavidin (1 : 300), or ALP-avidin (diluted by the manufacturer) for 1 h. The peroxidase reaction products were developed with 3,3′-diaminobenzidine and then counterstained with hematoxylin. The alkaline phosphatase reaction products were developed with a Dako Fuchsin Substrate-Chromogen System (Dako Ltd.) and counterstained with hematoxylin (21). For control studies on the antibodies, normal rabbit and rat IgGs were used instead of the primary antibodies. For control studies on ALP, the sections were incubated with the substrate solution with 1 mM levamisole.

Total RNA isolation and RT-PCR amplification of perlecan core mRNA

Total RNA was prepared from fresh surgical specimens by ISOGEN total RNA isolation reagent (Nippongene, Tokyo, Japan) according to the manufacturer's instructions. cDNAs were synthesized from the RNA with the SuperScript Pre-amplification System (Gibco-BRL, Grand Island, NY, USA). Following RT, PCR was carried out in an Astec thermal cycler PC-800 (Astec Co. Ltd., Fukuoka, Japan) as follows: the reaction products of the RT were diluted with 1× PCR buffer (50 mM KCl, 10 mM Tris–HCl (pH 8.5), 1.5 mM, and 0.01% Triton X-100) to a final volume of 50 μl, which contained 100 ng each of a forward oligonucleotide primer and a reverse primer, additional dNTPs (final concentration of 0.2 mM), and 2.5 U of Taq DNA polymerase (Takara Shuzo Co. Ltd., Kyoto, Japan). The oligonucleotide primers flanking the exon of domain I of perlecan core (nucleotide number 110–613, No. M77174, GenBank) were synthesized as follows: 5′-CATGGGCTGAGGGCATACG-3′, forward; and 5′-GTTCCGACGCCTGGGCACA-3′, reverse, to generate a 503-bp product. The thermocycling protocol during 35 amplification cycles was as follows: denaturation at 94°C for 1 min, annealing at 55°C for 1 min, extension at 72°C for 1 min, and termination with a final cycle: annealing (55°C for 1 min) and extension (72°C for 7 min). Exponential amplifications were confirmed in the 35 cycles. As an internal standard, the glyceraldehyde-3-phosphate dehydrogenase (GAPDH) gene was also amplified at the same time, as described elsewhere (11). The amplified DNA fragments were analyzed by electrophoresis on 2.5% agarose gels.

In situ *hybridization*

Expression of perlecan mRNA in radicular cyst walls was examined by an *in situ* hybridization technique (7). Perlecan RNA probes were prepared by a digoxigenin (DIG) RNA

labeling kit (Boehringer Mannheim GmbH, Mannheim, Germany) using SP6/T7 RNA polymerase (Promega Corporation, Madison, WI, USA). Template cDNA (1.5 kbp, corresponding to domain III of human perlecan core) was generously provided by Dr Karl Tryggvason (18). The cDNA was digested with *Eco*RI and *Sma*I, and then the resultant 700-bp fragment was ligated into the pSPT18 vector (Boehringer Mannheim GmbH). The vector plasmid was linearized by *Sma*I and transcribed with T7 RNA polymerase for the anti-sense probe and was linearized by *Eco*RI and transcribed with SP6 RNA polymerase for the sense probe.

Paraffin sections recovered in 0.05% diethyl pyrocarbonate (DEPC)-treated water were mounted on DEPC-treated slide glasses. After deparaffinization, the sections were washed with PBS and treated with 1 μg/ml of proteinase K (Sigma Chemical Co.) for 20 min at 37°C, followed by washing with 0.2% glycine in PBS. They were then dehydrated with a series of ethanol (70–100%) and air-dried. Hybridization was performed at 45°C for 16 h in a moist chamber. The hybridization solution contained 10 mM phosphate buffer (pH 7.4), 10% dextran sulfate, 1× Denhardt's solution, 100 μg/ml of salmon sperm DNA, 125 μg/ml of yeast tRNA, 3× SSC, 50% formamide, and 500 ng/ml of probe. After hybridization, the cover glasses were rinsed with 0.2 M maleic acid buffer (pH 7.5). Hybridization signals were visualized by using the DIG Nucleic Acid Detection Kit (Boehringer Mannheim GmbH), and sections were counterstained with methyl green.

Results

Histopathology

The cyst wall was composed of granulation tissue with an inner lining of squamous epithelium. The epithelial linings often disappeared because of inflammation. The granulation tissue just beneath the epithelial lining was usually associated with a dense infiltration of inflammatory cells. Towards the outer part, the granulation tissue of the cyst wall became fibrous (Fig. 1a). In the intermediate area between the fibrous layer and subepithelial layer with the inflammatory cells, there was a myxoid or edematous zone, which was filled with pale-stained amorphous and granular material, and eosinophilic collagen bundles were poorly formed. Such matrices appeared slightly metachromatic in toluidine blue staining (not shown). In these areas, inflammatory cells were mainly composed of macrophages as well as plasma cells and lymphocytes, and activated fibroblasts or endothelial cells with capillary formation were scattered. Foam cells were occasionally aggregated in this immature granulation tissue (Fig. 3a). In addition, there were cholesterol clefts surrounded by foreign body-type multinuclear giant cells within the granulation tissue layer (Fig. 4a). These cholesterol granulomas were often protruded into

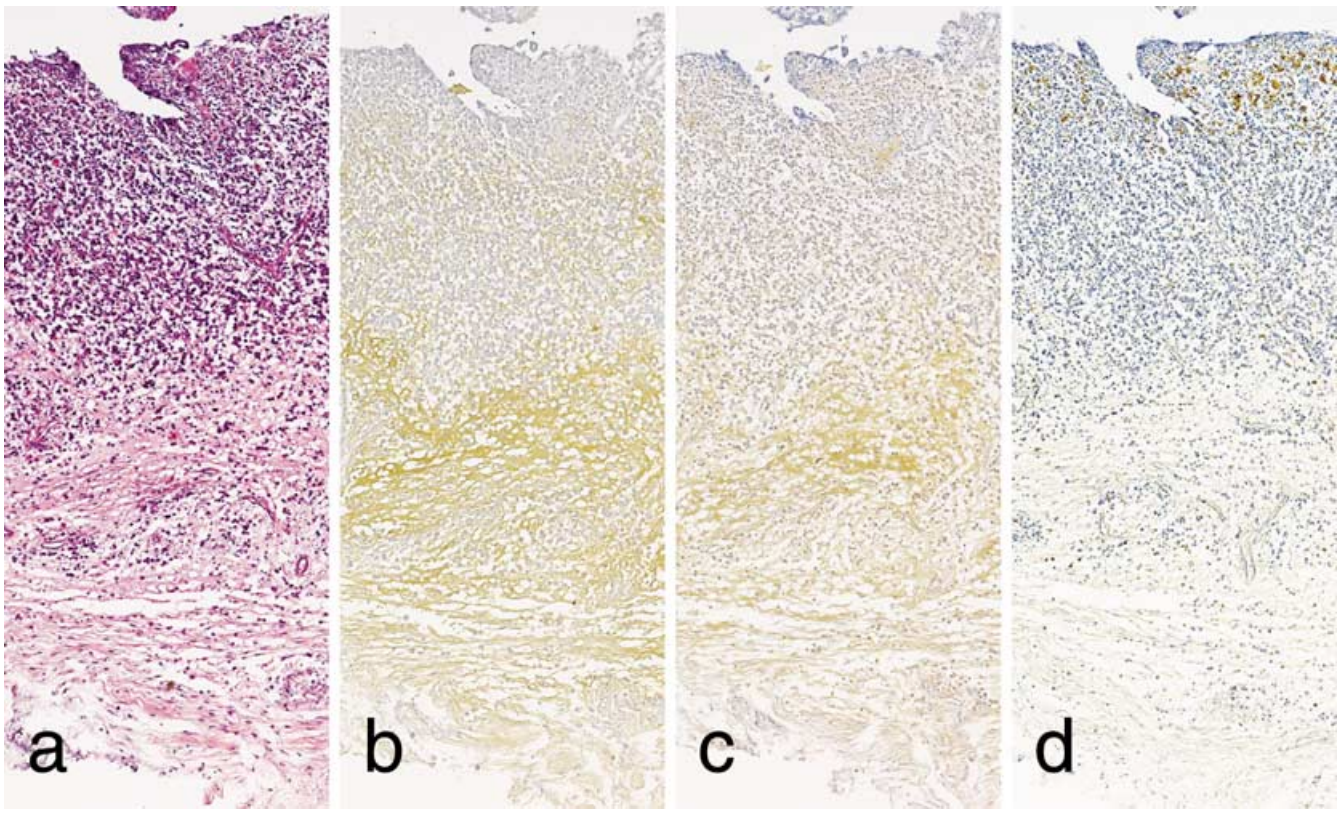

Figure 1 Radicular cyst wall of the jaw. (a) HE stain and (b) immunoperoxidase stains for perlecan, (c) for apo B, and (d) for CD68. Magnification ×50. Counterstained with hematoxylin. The cyst wall is composed of inner immature and outer fibrous granulation tissue layers. Just beneath the immature layer with a dense inflammatory cell infiltration, there is a myxoedematous layer, which is strongly immunoreactive for perlecan and apo B. CD68-positive macrophages are mainly localized in the inner part of the cyst wall.

the cystic lumen with ulcerated changes of the squamous epithelium-lined inner surface.

Immunohistochemistry

The myxoid or edematous matrices of the cyst wall were strongly immunopositive for perlecan (Figs. 1b and 2b) as well as for apo B (Fig. 1c). Their immunolocalization patterns were almost identical. Ox-LDL was immunolocalized in a similar fashion, but its staining intensity was weaker and the immunopositive area was less extensive (Fig. 2c). Smaller CD68-positive macrophages, which were widely distributed in the subepithelial layer and in the intermediate area (Figs. 1d and 3b), were also immunopositive for apo B (Fig. 3c) and Ox-LDL (Fig. 3d). However, larger foam cells, which were also positive for CD68 (Fig. 3b), were not always positive for apo B (Fig. 3c). Ox-LDL and apo B were also immunolocalized within the cytoplasm of plasma cells (not shown), although the stainings neither were expected nor have been described previously in the literature. There was no staining for perlecan, apo B, or Ox-LDL within the cholesterol clefts. CD68-positive foreign body-type multinuclear giant cells (Fig. 4b) surrounding the cholesterol clefts were not immunopositive for apo B (Fig. 4c) but were positive for Ox-LDL (Fig. 4d).

In situ *hybridization*

In situ hybridization signals for perlecan core protein mRNA were localized in fibroblastic spindle-shaped cells in the myxoedematous stroma (Fig. 5a). In addition, endothelial cells as well as pericytes of the capillaries and venules were positive for perlecan mRNA (Fig. 5b). These perlecan-positive cells had rather plump shapes with clear nuclei. The signals were localized diffusely within the cytoplasm. This indicated that perlecan in the myxoedematous stroma of the cyst wall was produced by these three kinds of cells.

RT-PCR

Total RNA was extracted from each fresh tissue specimen of radicular cysts, and 3 μg of each of them was reverse-transcribed with oligo-dT primers. The cDNAs were then amplified with the primer pairs for perlecan. PCR products of 503 bp were detected in all of the samples examined (Fig. 6). The relative amounts of PCR products for perlecan (503 bp) against GAPDH (983 bp) varied between radicular cyst cases (not shown). The results from the *in situ* hybridization and RT-PCR experiments indicated that perlecan was actively produced in the cyst wall granulation tissue.

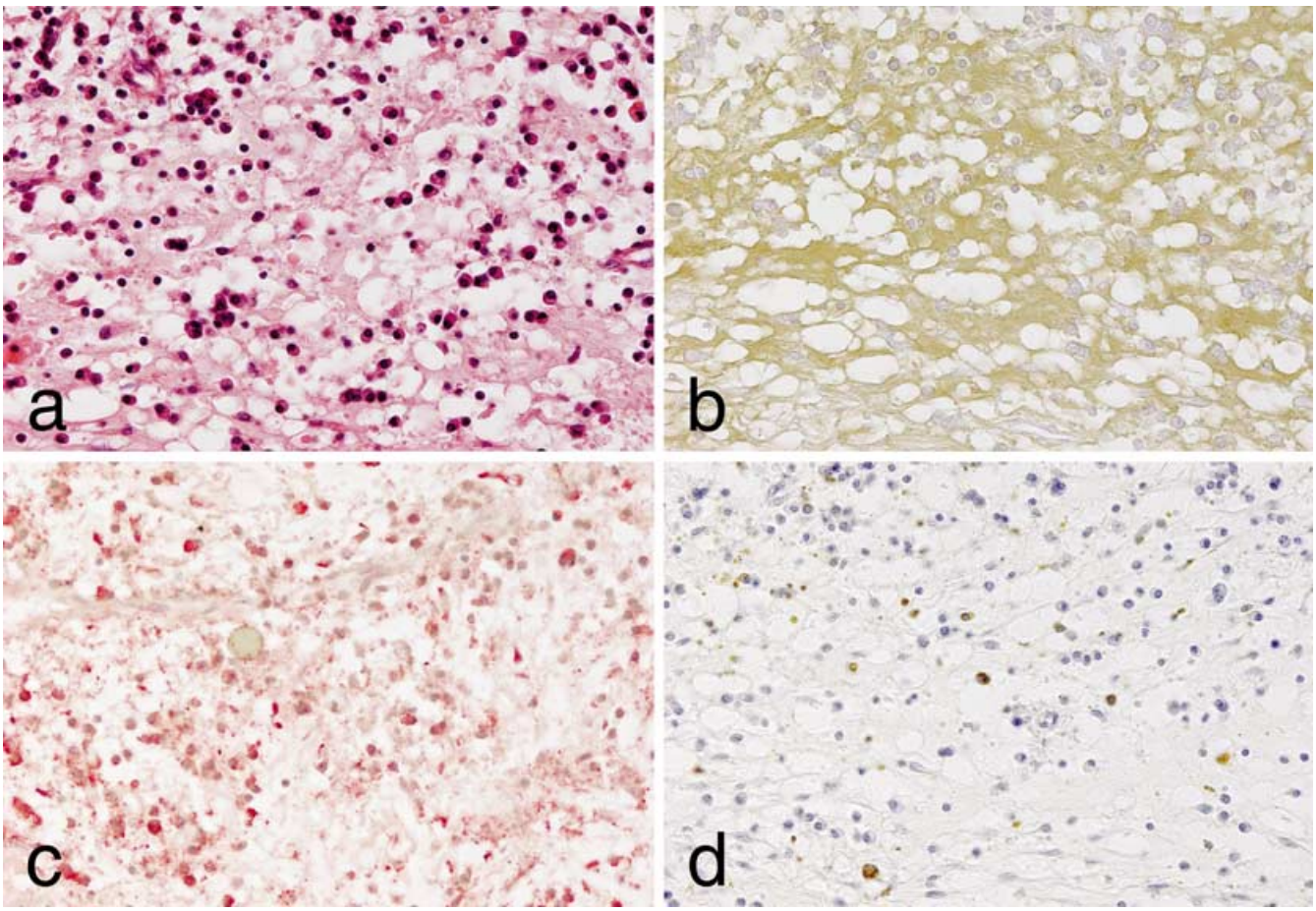

Figure 2 Higher magnification of myxoedematous stroma of radicular cyst wall. (a) HE stain, (b) immunoperoxidase stains for perlecan and (d) for CD68, and (c) immunoalkaline phosphatase stain for Ox-LDL. Magnification ×250. Counterstained with hematoxylin. Myxoid stroma is also immunopositive for Ox-LDL in addition to macrophages.

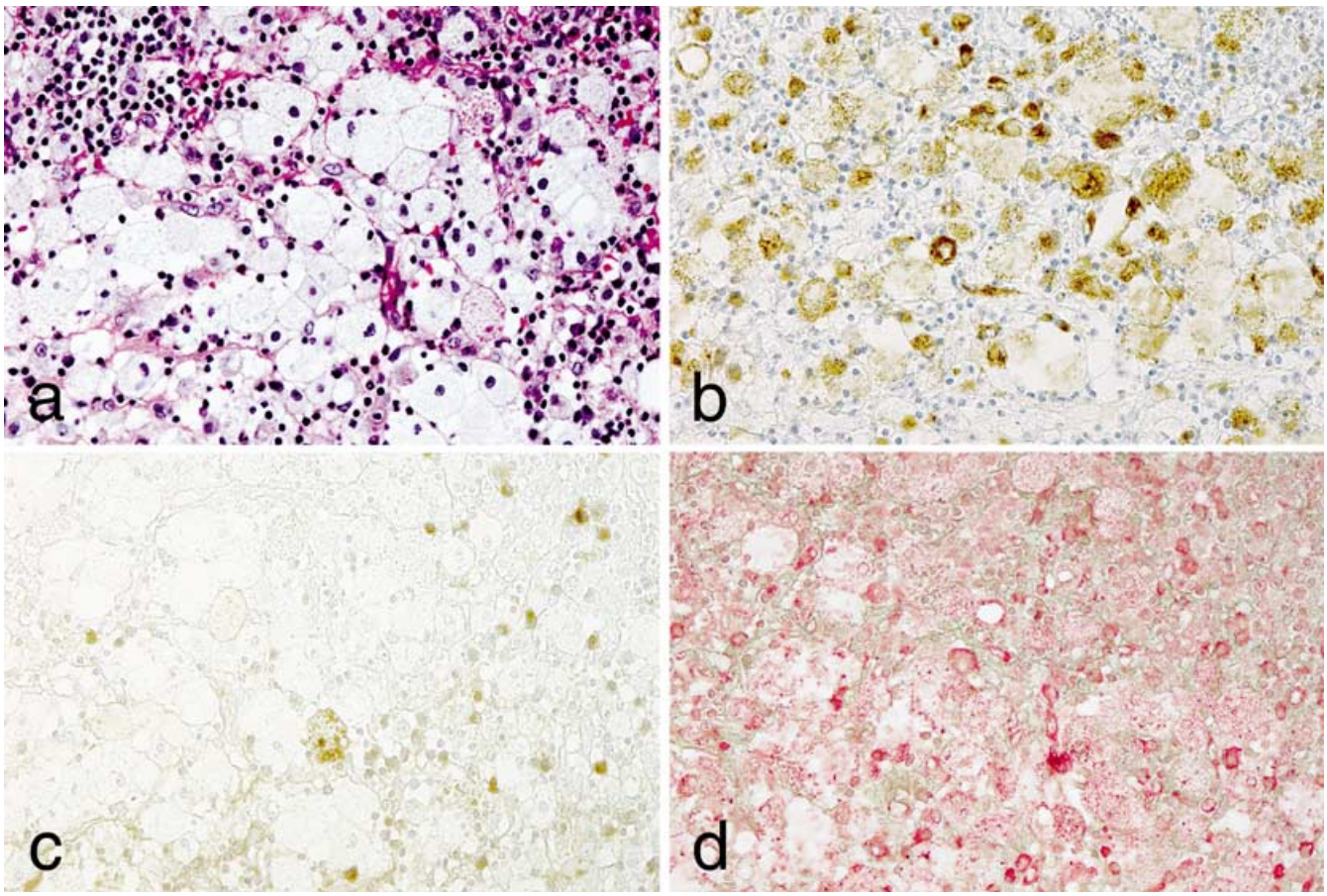

Figure 3 Macrophages and their foamy forms in the immature granulation tissue of radicular cyst wall. (a) HE stain, (b) immunoperoxidase stains for CD68 and (c) and for apo B, and (d) immunoalkaline phosphatase stain for Ox-LDL. Magnification ×200. Counterstained with hematoxylin. Foamy cells are immunopositive for Ox-LDL, but not always for apo B.

Discussion

In the present study, we were able to successfully demonstrate for the first time the immunohistochemical co-localization of perlecan and LDL/Ox-LDL in the wall of radicular cysts. This result suggests that condensation and crystallization of cholesterol within the cyst wall partly result from the binding of LDL to stromal perlecan, which is synthesized by at least three kinds of stromal cells of granulation tissues. The cystic lumen contains cholesterol-rich fluids, which are believed to be derived from the vascular circulation or from local metabolic products of cyst wall granulation tissues (1–3, 22–24). However, little is currently known about the molecular mechanism for cholesterol granuloma formation in the cyst wall. The present results might explain the possible pathogenesis of cholesterol granulomas, which seems to be one of the driving forces for growth of jaw cysts, especially those with inflammatory backgrounds (1, 3).

Perlecan possesses three major heparan sulfate (HS) chains on a large core protein of about 470 kDa in size. Its core protein consists of five distinct domains: the first domain contains three Ser–Gly–Asp sequences, which are potential attachment sites for HS side chains; domain II has four LDL receptor-like repeats; domain III contains laminin short arm-like repeats; domain IV has neural cell adhesion molecule (NCAM)-like repeats; and domain V contains laminin A chain-like repeats and EGF motifs (17, 18). The role of HS chains has been extensively studied, especially in terms of their binding with various growth factors (25). On the other hand, the functional roles of the core protein are poorly understood despite its multidomain structure, suggesting the multifunctional properties of this molecule (26). The LDL receptor-like structure in domain II is composed of ∼40 amino acid residue-long repeats that have high sequence similarity with those in the ligand-binding region of the LDL receptors (17). These repeats are very hydrophilic and contain a consensus sequence with six conserved cysteines and negatively charged acidic residues, which are characteristic of the ligand-binding regions of the LDL receptors. It is thus suggested that LDL molecules bind to perlecan via apo B–domain II interaction. However, there has been no direct demonstration of the binding of these two molecules in any pathophysiologic situations, and no attempt has ever been made to investigate it.

There has been only one comprehensive investigation on glycosaminoglycans of the odontogenic cyst wall, which was by Smith et al. (27). The intention of this study was to determine the source of glycosaminoglycans in cyst fluids, which also had been found in their previous study (28). They demonstrated histochemically that glycosaminoglycans,

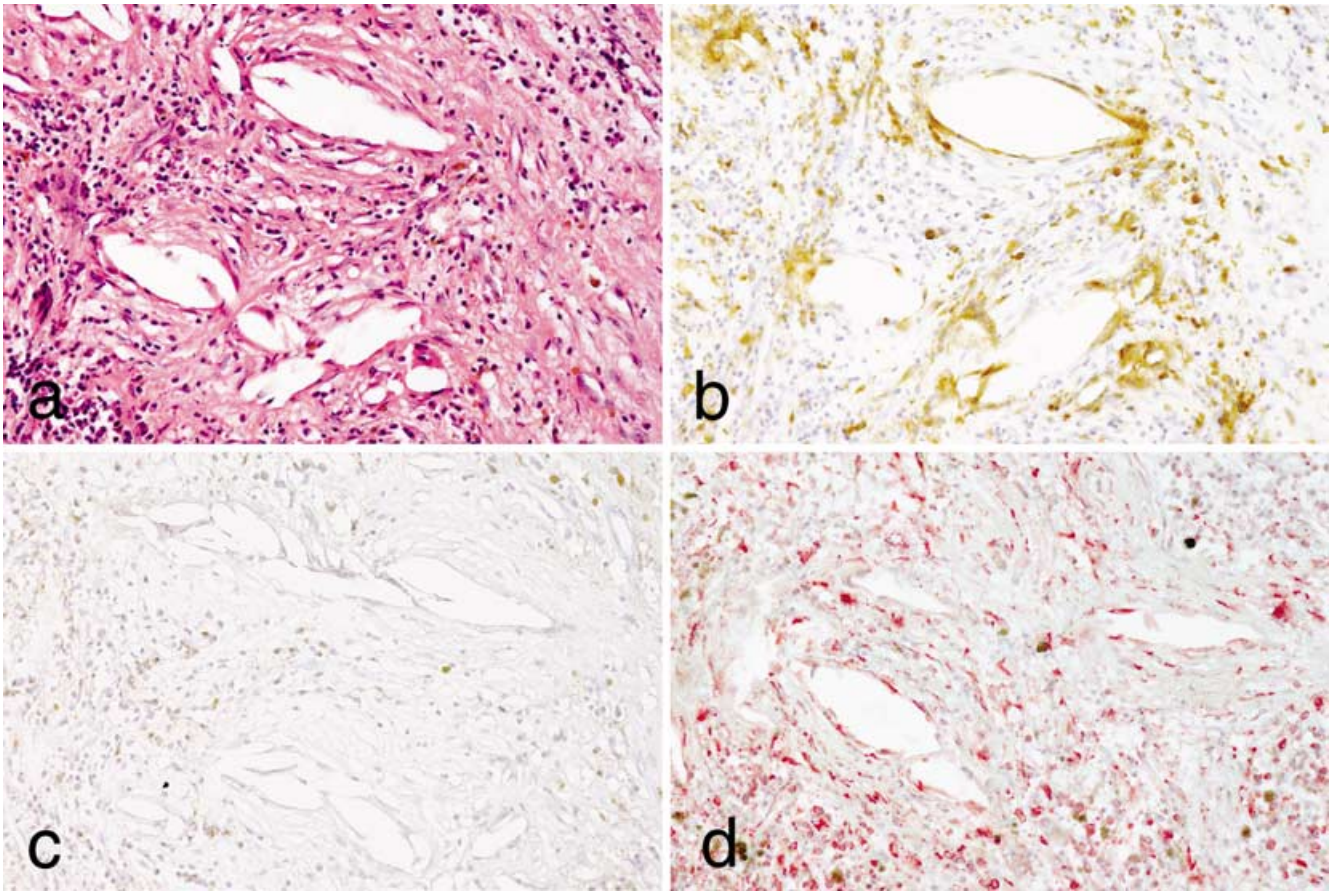

Figure 4 Cholesterol clefts surrounded by multinuclear giant cells in radicular cyst wall. (a) HE stain, (b) immunoperoxidase stains for CD68 and (c) for apo B, and (d) immunoalkaline phosphatase stain for Ox-LDL. Magnification ×125. Counterstained with hematoxylin. Foreign body-type giant cells surrounding cholesterol clefts are not immunopositive for apo B but are positive for Ox-LDL.

including hyaluronic acid, heparin/HS, and chondroitin sulfate exist in the cyst wall, especially in the subepithelial connective tissue, suggesting that those in the luminal fluids are released from cyst wall connective tissues, and that the fluids are important in the expansile growth of cysts. In addition, they discussed the difficulty of determining the origin of heparin/HS deposited in the cyst wall and concluded that mast cells were responsible for the deposit because HS is not normally found in the stroma but on the cell surface or in the basement membrane. However, it is

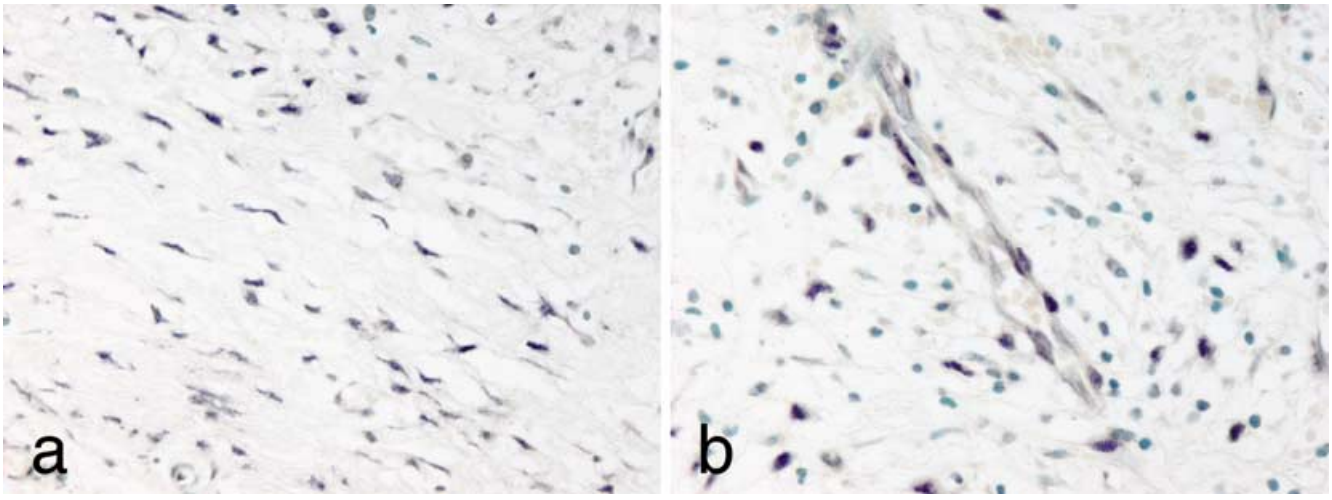

Figure 5 *In situ* hybridization for perlecan mRNA in radicular cyst wall. Immunoalkaline phosphatase stain with DIG-labeled RNA probes. Counterstained with methyl green. Magnification (a) ×250 and (b) ×300. Perlecan mRNA signals are detected in fibroblasts, endothelial cells, and pericytes in the myxoid granulation tissue.

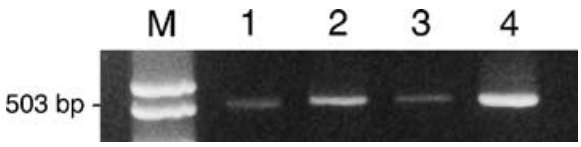

Figure 6 RT-PCR for perlecan mRNA of radicular cyst walls. Lane M, molecular weight standard; and lanes 1–4, surgical specimens of radicular cyst. A PCR product of 503 bp is obtained in varying degrees, and synthesis of perlecan core protein is confirmed.

now accepted that perlecan is expressed more widely than previously expected in neoplastic (4–12) as well as in granulation tissues (13–15). Although we have not determined the contents of HS in cyst fluids, it should be obvious that at least HS chains are derived from granulation tissues of the cyst wall and that proteoglycans with HS chains are of the basement membrane-type biosynthesized by the three types of stromal cells in the cyst wall.

As to the accumulation of cholesterol in cyst fluids, Yashima et al. (24) reported that heat-stable cholesterol-binding protein, which originates from apo B, itself plays an important role in the process. The origin of the cyst fluid cholesterol was suggested to be serum LDL by Skaug (22) and Suzuki (2). Suzuki also demonstrated that cholesterol crystals were composed of only free cholesterol, which could be esterified by lecithin-cholesterol acyltransferase. As the cyst fluids contain no such enzymatic activity, free cholesterol is expected to crystallize in the cyst wall (23). Our present result demonstrating that apo B and Ox-LDL are not always immunolocalized in cholesterol clefts surrounded by foreign body giant cells should support his hypothesis. Also from this result, it is suggested that free cholesterol for crystallization originated from foamy macrophages because they accumulated only the lipid portion of LDL molecules in their cytoplasm. The absence of apo B in macrophages suggests that the protein part of LDL is much more quickly metabolized within them.

In the present study, the myxoid or edematous matrices in immature granulation tissues were shown to be simultaneously immunopositive for perlecan and apo B/Ox-LDL. As such kinds of tissues with myxoid appearances have been shown to be rich in perlecan (4, 5, 9–14), it is reasonable to assume that LDL molecules may easily be trapped in the myxoid stroma. As Ox-LDL was also immunolocalized in the myxoid stroma, as well as in the cytoplasm of foamy macrophages, oxidized forms of LDL molecules are suggested to play a pathogenic role in the local circumstances of the cyst wall, although it remains unknown where they are oxidized. The localizations of apo B and Ox-LDL were not always identical. Although apo B was also demonstrated in a small number of foam cells, it was mainly localized in the extracellular matrix with a wider spread in comparison to Ox-LDL. On the other hand, Ox-LDL was distributed mostly in foam cells. This suggests that most of the foamy macrophages lost the protein part (apo B) of LDL but still preserved the lipid part (Ox-LDL), signifying that metabolisms between apo B and lipids are different in the foam cells. On the other hand, the antibody DLH3 stains the foam cells strongly because DLH3 recognizes oxidized phosphatidylcholine produced by oxidation of the lipid part and peptides (mainly apo B) modified by oxidized phosphatidylcholine (20). Thus, it is likely that LDL molecules are oxidized after their binding to the stroma.

It has been well documented that in human arteriosclerotic foci, LDL interacts with vascular wall extracellular matrix molecules, including proteoglycans, which are derived from endothelial cells and smooth muscle cells (29, 30). Among the proteoglycans, dermatan sulfate or chondroitin sulfate proteoglycans have been shown to be able to bind LDL more efficiently than HSPGs do (29), and the contents of these two proteoglycans and of hyaluronic acid are larger than that of HSPGs in the atherosclerotic vascular walls (30). Pillarisetti (31) also concluded a negative relationship between HSPG and atherosclerosis but instead suggested that HSPG has potential anti-atherogenic functions. Recently, however, a totally opposite result has been found demonstrating that there is accumulation of perlecan and biglycan, not versican, corresponding to the localization of apo B in murine atherosclerotic lesions (32). Thus, it is still controversial which proteoglycans are ligands for LDL in atherosclerotic processes, which should be basically similar to the inflammatory conditions in the cyst wall. However, it seems obvious that adherence of LDL to arterial proteoglycans increases LDL's susceptibility to oxidation *in vitro* (33) and that prior oxidation of LDL does not enhance its retention in arteries (34). Therefore, these data would support our speculation that LDL from the circulation is first trapped by perlecan in the cyst wall granulation tissue and then is oxidized in the local milieu to be internalized by macrophages via scavenger receptors. As to the origin of cholesterol crystals, it is reported that cholesterol crystals are found within foam cells in atherosclerotic foci and that their death by necrotic or apoptotic processes contributes to lipid core formation and crystallization in the extracellular space (35, 36).

In conclusion, the present data suggest that LDL entrapped by perlecan is accumulated and oxidized in the extracellular space, and that Ox-LDL is scavenged by macrophages and is primarily deposited intracellularly, then the macrophages are converted into lipid-laden foamy cells. These foamy cells may finally rupture and release the lipids concentrated in their cytoplasm into the extracellular space. Following this, concentrated free cholesterol results in crystallization. Cholesterol crystals in turn cause foreign body reactions to extend inflammatory reactions for cystic growth.

References

1. Shear M. *Cyst of the Oral Regions*, 3rd edn. Oxford: Wright, 1992; 157–9.
2. Suzuki M. A biological chemistry study on the nature of jaw cysts on the maintenance of homeostasis in jaw cyst fluid. *J Maxillofac Surg* 1975; **3**: 106–18.
3. Shear M. Cholesterol in dental cysts. *Oral Surg Oral Med Oral Pathol* 1963; **16**: 1465–73.
4. Saku T, Cheng J, Okabe H, Koyama Z. Immunolocalization of basement membrane molecules in the stroma of salivary gland pleomorphic adenoma. *J Oral Pathol Med* 1990; **19**: 208–14.
5. Cheng J, Saku T, Okabe H, Furthmayr H. Basement membranes in adenoid cystic carcinoma. *Cancer* 1992; **69**: 2631–40.

6. Cheng J, Irié T, Munakata R, et al. Biosynthesis of basement membrane molecules by salivary adenoid cystic carcinoma cells. *Virchows Arch* 1995; **426**: 577–86.
7. Kimura S, Cheng J, Toyoshima K, Oda K, Saku T. Basement membrane heparan sulfate proteoglycan (perlecan) synthesized by ACC3, adenoid cystic carcinoma cells of human salivary gland origin. *J Biochem* 1999; **125**: 406–13.
8. Kimura S, Cheng J, Ida H, Hao N, Fujimori Y, Saku T. Perlecan (heparan sulfate proteoglycan) gene expression reflect in the characteristic histological architecture of salivary adenoid cystic carcinoma. *Virchows Arch* 2000; **437**: 122–8.
9. Ida-Yonemochi H, Ikarashi T, Nagata M, Hoshina H, Takagi R, Saku T. The basement membrane-type heparan sulfate proteoglycan (perlecan) in ameloblastomas: its intercellular localization in stellate reticulum-like foci and biosynthesis by tumor cells in culture. *Virchows Arch* 2002; **441**: 165–73.
10. Ikarashi T, Ida-Yonemochi H, Ohshiro K, Cheng J, Saku T. Intraepithelial expression of perlecan, a basement membrane-type heparan sulfate proteoglycan reflects dysplastic changes of the oral mucosal epithelium. *J Oral Pathol Med* 2004; **33**: 87–95.
11. Sabit H, Tsuneyama K, Shimonishi T, et al. Enhanced expression of basement-membrane-type heparan sulfate proteoglycan in tumor fibro-myxoid stroma of intrahepatic cholangiocarcinoma. *Pathol Int* 2001; **51**: 248–56.
12. Munakata R, Irié T, Cheng J, Nakajima T, Saku T. Pseudocyst formation by adenoid cystic carcinoma cells in collagen gel culture and in SCID mice. *J Oral Pathol Med* 1996; **25**: 441–8.
13. Murata M, Hara K, Saku T. Dynamic distribution of basic fibroblast growth factor during epulis formation: an immunohistochemical study in an enhanced healing process of the gingiva. *J Oral Pathol Med* 1997; **26**: 224–32.
14. Ohtani H, Nakamura S, Watanabe Y, Mizoi T, Saku T, Nagura H. Immunocytochemical localization of basic fibroblast growth factor in carcinomas and inflammatory lesions of the human. *Lab Invest* 1993; **68**: 520–7.
15. Metwaly H, Cheng J, Ida-Yonemochi H, et al. Vascular endothelial cell participation in formation of lymphoepithelial lesions (epi-myoepithelial islands) in lymphoepithelial sialadenitis (benign lymphoepithelial lesion). *Virchows Arch* 2003; **443**: 17–27.
16. Ikada Y, Suzuki M, Iwata H. Water in mucopolysaccharides. In: Roeland SP, ed. *Water in Polymers.* Washington, DC: The American Chemical Society, 1979; 287.
17. Murdoch AD, Dodge GR, Cohen I, Tuan RS, Iozzo RV. Primary structure of the human heparan sulfate proteoglycan from basement membrane (HSPG2/Perlecan). *J Biol Chem* 1992; **267**: 8544–57.
18. Kallunki P, Tryggvason K. Human basement membrane heparan sulfate proteoglycan core protein: a 467-kD protein containing multiple domains resembling elements of the low density lipoprotein receptor, laminin, neural cell adhesion molecules, and epidermal growth factor. *J Cell Biol* 1992; **116**: 559–71.
19. Saku T, Furthmayr H. Characterization of the major heparan sulfate proteoglycan secreted by bovine aortic endothelial cells in culture. *J Biol Chem* 1989; **264**: 3514–23.
20. Itabe H, Takeshima E, Iwasaki H, et al. A monoclonal antibody against oxidized lipoprotein recognizes foam cells in atherosclerotic lesions. Complex formation of oxidized phosphatidylcholines and polypeptides. *J Biol Chem* 1994; **269**: 15274–9.
21. Jimi S, Saku K, Kusaba H, Itabe H, Koga N, Takebayashi S. Deposition of oxidized low-density lipoprotein and collagenosis occur coincidentally in human coronary stenosis: an immunohistochemical study of atherectomy. *Coron Artery Dis* 1998; **9**: 551–7.
22. Skaug N. Lipoproteins in fluid from non-keratinizing jaw cysts. *Scand J Dent Res* 1976; **84**: 98–105.
23. Suzuki M. A biochemical study of the nature of jaw cysts (II). *J Maxillofac Surg* 1984; **12**: 213–24.
24. Yashima M, Ogura N, Abiko Y. Studies on cholesterol accumulation in radicular cyst fluid – origin of heat-stable cholesterol-binding protein. *Int J Biochem* 1990; **22**: 165–9.
25. Iozzo RV. Matrix proteoglycans: from molecular design to cellular function. *Annu Rev Biochem* 1998; **67**: 609–52.
26. Olsen BR. Life without perlecan has its problems. *J Cell Biol* 1999; **147**: 909–11.
27. Smith G, Smith AJ, Browne RM. Histochemical studies on glycosaminoglycans of odontogenic cysts. *J Oral Pathol* 1988; **17**: 55–9.
28. Smith G, Smith AJ, Browne RM. Glycosaminoglycans in fluid aspirates from odontogenic cysts. *J Oral Pathol* 1984; **13**: 614–21.
29. Williams KJ, Tabas I. The response-to-retention hypothesis of early atherogenesis. *Arterioscler Thromb Vasc Biol* 1995; **15**: 551–61.
30. Wight TN. Cell biology of arterial proteoglycans. *Arteriosclerosis* 1989; **9**: 1–20.
31. Pillarisetti S. Lipoprotein modulation of subendothelial heparan sulfate proteoglycans (perlecan) and atherogenicity. *Trends Cardiovasc* 2000; **10**: 60–5.
32. Kunnjathoor VV, Chiu KD, O'Brien KD, LeBoeuf RC. Accumulation of biglycan and perlecan, but not versican, in lesions of murine models of atherosclerosis. *Arterioscler Thromb Vasc Biol* 2002; **22**: 462–8.
33. Camejo G, Hurt-Camejo E, Olsson U, Bondjers G. Proteoglycans and lipoproteins in atherosclerosis. *Curr Opin Lipidol* 1993; **4**: 385–91.
34. Chang MY, Lees AM, Lees RS. Low-density lipoprotein modification and arterial wall accumulation in a rabbit model of atherosclerosis. *Biochemistry* 1993; **32**: 8518–24.
35. Ball RY, Stowers EC, Burton JH, Cary NRB, Skepper JN, Mitchinson MJ. Evidence that the death of macrophage foam cells contributes to the lipid core of atheroma. *Atherosclerosis* 1995; **114**: 45–54.
36. Hegyi L, Skepper JN, Cary NRB, Mitchinton MJ. Foam cell apoptosis and the development of the lipid core of human atherosclerosis. *J Pathol* 1996; **180**: 423–9.

Acknowledgements

The authors wish to thank Dr K. Tryggvason for generously supplying the cDNA fragment of human perlecan core protein. This work was supported in part by Grants-in-Aid for Scientific Research from Japan Society for the Promotion of Science.